

Right-handed current contributions in $B \rightarrow K\pi$ decays

Kihyeon Cho* and Soo-hyeon Nam†

National Institute of Supercomputing and Networking, KISTI, Daejeon 305-806, Korea

(Dated: October 23, 2018)

We reexamine the right-handed current effects in $b \rightarrow s$ transitions in nonmanifest left-right models. Using the effective Hamiltonian approach including all possible low-energy operators, we obtain especially the $B \rightarrow K\pi$ decay amplitudes including annihilation contributions, and investigate the right-handed current contributions to CP asymmetries in $B \rightarrow K\pi$ decays. Taking into account the constraints from global analysis of muon decay measurements, $|V_{ub}|$ measurements in inclusive and exclusive B decays, and $B_s^0 - \bar{B}_s^0$ mixing measurements, we find the allowed regions of new physics parameters satisfying the current experimental data.

I. INTRODUCTION

CP asymmetry measurements in nonleptonic $b \rightarrow s$ decays have been receiving considerable attention over the past several years since the recent experimental measurements in some decay channels are in disagreement with naive estimates of the Standard Model (SM). One of the important examples is the direct CP asymmetries in $B \rightarrow K\pi$ decays [1]. Current world averages of the CP asymmetries in $B \rightarrow K\pi$ decays are given by [2]:

$$\begin{aligned} A_{CP}(B^0 \rightarrow K^\pm \pi^\mp) &= -0.086 \pm 0.007, \\ A_{CP}(B^\pm \rightarrow K^\pm \pi^0) &= 0.040 \pm 0.021, \\ A_{CP}(B^\pm \rightarrow K^0 \pi^\pm) &= -0.015 \pm 0.012. \end{aligned} \quad (1)$$

However, the naive factorization assumption predicts $A_{CP}(B^0 \rightarrow K^\pm \pi^\mp) \approx A_{CP}(B^\pm \rightarrow K^\pm \pi^0)$ [3], which is inconsistent with the current data in Eq. (1). This discrepancy can be explained by enhancing the smaller diagrams such as C' and P'_{EW} with a sizable strong phase through the SM fit to the $K\pi$ data [4], where C' and P'_{EW} stand for the color-suppressed tree and electroweak penguin amplitudes, respectively, in the topological decomposition [5]. Nonetheless, such enhancement of subdominant diagrams in the SM is not fully understood theoretically and also may not be sufficient to resolve other puzzles simultaneously in the B meson system [1]. Alternatively to the SM fit, since the prediction given in Ref. [3] did not incorporate all possible hadronic uncertainties, these decay modes have been also studied within the SM in the framework of different factorization approaches such as QCD factorization [6], perturbative QCD (PQCD) [7], and soft-collinear effective theory [8]. Even under such factorization assumptions, however, the above data have not been fully explained as well. In the SM, the sizes and patterns of CP violation in various decay modes are governed by a single complex phase which resides in the Cabibbo-Kobayashi-Maskawa (CKM) matrix, but such large CP violation effects have not been simply explained with this single parameter in any of those factorization methods in various decay modes simultaneously. Therefore, there has been several efforts to understand such large CP asymmetries beyond the SM with additional CP odd parameters [9]. Similarly in this paper, we study the new physics (NP) contributions to the direct CP asymmetries in $B \rightarrow K\pi$ decays as well as to (semi-)leptonic B decays and B mixing where NP effects could be sizable. In order to minimize hadronic uncertainties, we consider all relevant tree and penguin contributions even including annihilation types by adopting PQCD approach, and estimate the possible NP contributions.

One of the simplest extensions of the SM corresponding to such a scenario with additional CP phases is the nonmanifest ($V^R \neq V^L$) left-right model (LRM) with gauge group $SU(2)_L \times SU(2)_R \times U(1)$ where $V^L(V^R)$ is the left(right)-handed quark mixing matrix [10]. Since the LRM has the extended group $SU(2)_R$, there are new parameters such as a right-handed gauge coupling g_R , new charged (neutral) gauge bosons W_R (Z_R), and the $W_L - W_R$ ($Z_L - Z_R$) mixing angle ξ (η). After spontaneous symmetry breaking, the gauge eigenstates W_R mix with W_L to form the mass eigenstates W and W' with masses M_W and $M_{W'}$, respectively. Similarly, the neutral gauge bosons mix each other [11], but we do not present them here because Z_R contribution to flavor-changing B decays is negligible. Although tree-level flavor-changing neutral Higgs bosons with masses M_H enter into our theory due to gauge invariance, we also neglect their contributions by assuming $M_H \gg M_{W'}$ [12]. The mixing angle ξ and the ratio ζ of M_W^2 to $M_{W'}^2$,

*Electronic address: cho@kisti.re.kr

†Electronic address: glvnsh@gmail.com

are restricted by a number of low-energy phenomenological constraints [13]. One of the most stringent bounds on $M_{W'}$ was obtained from $K_L - K_S$ mixing. If the model has manifest ($V^R = V^L$) left-right symmetry ($g_R = g_L$) where $V^L(V^R)$ is the left(right)-handed quark mixing matrix, $M_{W'} > 2.5$ TeV [14]. Similar bounds were obtained recently by CMS and ATLAS from direct searches for the decay channels of the extra gauge bosons $W' \rightarrow \ell\nu$ under various assumptions on the right-handed neutrino masses and gauge couplings [15]. However, the form of V^R is not necessarily restricted to manifest or pseudomanifest ($V^R = V^{L*}K$) symmetric-type, where K is a diagonal phase matrix [10]. If V^R takes one of the following forms, the W_R mass limit can be significantly lowered [13], and V_{ub}^R can be as large as λ (for $M_{W_R} \geq 800$ GeV) [16]:

$$\begin{pmatrix} 1 & 0 & 0 \\ 0 & 0 & 1 \\ 0 & 1 & 0 \end{pmatrix}, \quad \begin{pmatrix} 0 & 1 & 0 \\ 1 & 0 & 0 \\ 0 & 0 & 1 \end{pmatrix}, \quad \begin{pmatrix} 0 & 1 & 0 \\ 0 & 0 & 1 \\ 1 & 0 & 0 \end{pmatrix}. \quad (2)$$

As well as the CP-violating observables in $B \rightarrow K\pi$ decays, we also accommodate a large CP-violating phase in B_s mixing observed at Tevatron and a disagreement emerged between the determination of $|V_{ub}|$ from inclusive and exclusive B decays [17]. In order to incorporate all of those considerations, we take the following form of V^R as similarly done in Ref. [18]:

$$V^R = \begin{pmatrix} \sim 0 & c_R e^{i\alpha_1} & s_R e^{i\alpha_2} \\ e^{i\omega} & \sim 0 & \sim 0 \\ \sim 0 & -s_R e^{i\alpha_3} & c_R e^{i\alpha_4} \end{pmatrix}, \quad (3)$$

where c_R (s_R) $\equiv \cos\theta_R$ ($\sin\theta_R$) ($0^\circ \leq \theta_R \leq 90^\circ$). Here the matrix elements indicated as ~ 0 may be $\lesssim 10^{-2}$ and unitarity requires $\alpha_1 + \alpha_4 = \alpha_2 + \alpha_3$. Especially, with this form, the present experimental measurement of the large branching fractions for $B \rightarrow \tau\nu$ decays can be explained [17, 18], but the right-handed current effect in B_d mixing is negligible so we only consider direct CP asymmetries in $B \rightarrow K\pi$ decays. One can of course take different types of V^R without taking into account of $|V_{ub}^R|$, and relevant studies were done earlier in Refs. [19, 20].

This paper is organized as follows. In Sec. II, we briefly discuss some of phenomenological constraints without assuming manifest (or pseudomanifest) left-right symmetry. We present the effective Hamiltonian describing $\Delta B = 1$ and $\Delta S = 1$ transition in Sec. III, and obtain $B \rightarrow K\pi$ decay amplitudes including all relevant tree and penguin contributions in the general LRM in Sec. IV. In Sec. V, we explicitly show the allowed regions of NP parameters satisfying the current experimental data, taking into account all the constraints obtained in Sec. II. Finally, we conclude in Sec. VI.

II. PHENOMENOLOGICAL CONSTRAINTS

We consider the case that W' masses are not too heavy so that it can be accessible at LHC. Without assuming manifest or pseudomanifest left-right symmetry in the general LRM, W' masses are not highly constrained by low-energy electroweak measurements, but still W' exchange effects could be seen in various decay modes, and the bound of its mass could be obtained independent of the form of V^R . For instance, we can obtain the lower bound on $M_{W'}$ from global analysis of muon decay measurements as follows [21]:

$$\zeta_g < 0.017 \quad \text{or} \quad M_{W'} > (g_R/g_L) \times 620 \text{ GeV}. \quad (4)$$

where $\zeta_g \equiv g_R^2 M_W^2 / g_L^2 M_{W'}^2$. In general, $\zeta_g \geq \xi_g \equiv (g_R/g_L)\xi$ for ordinary Higgs representations [13, 22].

As well as $M_{W'}$ and ξ_g , we have additional NP parameters such as θ_R and α_i in the quark sector as shown in Eq. (3) in the general LRM. Among those new parameters, θ_R and α_2 can be constrained by the disagreement emerged between the determination of $|V_{ub}|$ from inclusive and exclusive B decays. $|V_{ub}|$ determined in exclusive B decays is related to $|V_{ub}^L|$ in the LRM as

$$|V_{ub}|_{excl} = |V_{ub}^L| |1 + \xi_u| \simeq |V_{ub}|_{incl} |1 + \xi_u|, \quad (5)$$

where $\xi_q \equiv \xi(g_R V_{qb}^R) / (g_L V_{qb}^L)$ and $q = u, c$ [17]. From the mismatch between the values of $|V_{ub}|$ extracted from inclusive and exclusive B decays, we roughly obtain the following 2σ bound:

$$-1.55 < \xi_g s_R \cos(\alpha_2 + \gamma) \times 10^3 < 0.41, \quad (6)$$

where $\gamma = 68^\circ$.

In Eq. (3), α_3 and α_4 are constrained by $B_s^0 - \bar{B}_s^0$ mixing measurements. The dispersive part of the $B_s^0 - \bar{B}_s^0$ mixing matrix element in the LRM can be written as

$$M_{12}^s = M_{12}^{SM} + M_{12}^{LR} = M_{12}^{SM} (1 + r_{LR}^s), \quad (7)$$

where

$$r_{LR}^s \equiv \frac{M_{12}^{LR}}{M_{12}^{SM}} = \frac{\langle \bar{B}_s^0 | H_{eff}^{LR} | B_s^0 \rangle}{\langle \bar{B}_s^0 | H_{eff}^{SM} | B_s^0 \rangle}, \quad (8)$$

and the explicit form of the effective Hamiltonians H_{eff}^{SM} and H_{eff}^{LR} describing the $\Delta B = 2$ transition in the LRM can be found in Refs. [20, 22]. Following the factorization methods used in Ref. [20] with the given form of V^R in Eq. (3), we obtain the right-handed current contributions to $B_s^0 - \bar{B}_s^0$ mixing as

$$r_{LR}^s \approx 162 \left(\frac{1 - 5.03\zeta_g - (0.490 - 1.96\zeta_g) \ln(1/\zeta_g)}{1 - 10.2\zeta_g + 30.1\zeta_g^2} \right) \zeta_g s_R c_R e^{-i(\alpha_3 - \alpha_4)} + 1.70 \xi_g s_R e^{-i\alpha_3}. \quad (9)$$

The deviation of the present experimental data from the SM predictions on B_s meson mixing gives the following 2σ bound [23]:

$$0.86 < |1 + r_{LR}^s| < 1.22, \quad (10)$$

and we will use this bound together with those in Eqs. (4) and (6) for our numerical analysis in Sec V.

III. EFFECTIVE HAMILTONIAN

In order to include QCD effects systematically, we start from the following low-energy effective Hamiltonian describing $\Delta B = 1$ and $\Delta S = 1$ transition as done similarly in Ref. [19]:

$$\mathcal{H}_{eff} = \frac{G_F}{\sqrt{2}} \left[\sum_{\substack{i=1,2,11,12 \\ q=u,c}} \lambda_q^{LL} C_i^q O_i^q - \lambda_t^{LL} \left(\sum_{i=3}^{10} C_i O_i + C_7^\gamma O_7^\gamma + C_8^G O_8^G \right) \right] + (C_i O_i \rightarrow C_i' O_i'), \quad (11)$$

where $\lambda_q^{AB} \equiv V_{qs}^{A*} V_{qb}^B$, $O_{1,2}$ are the standard current-current operators, $O_3 - O_{10}$ are the standard penguin operators, and O_7^γ and O_8^G are the standard photonic and gluonic magnetic operators, respectively, which can be found in Ref. [24]. In addition to those SM operators, in the LRM, the operator basis is doubled by O_i' which are the chiral conjugates of O_i . Also new operators $O_{11,12}$ and $O_{11,12}'$ arise with mixed chiral structure of $O_{1,2}$ and $O_{1,2}'$ as follows:

$$O_{11}^q = (\bar{s}_\alpha q_\beta)_{V-A} (\bar{q}_\beta b_\alpha)_{V+A}, \quad O_{12}^q = (\bar{s}_\alpha q_\alpha)_{V-A} (\bar{q}_\beta b_\beta)_{V+A}, \quad (12)$$

where $(V \pm A)$ refers to the Lorentz structure $\gamma_\mu (1 \pm \gamma_5)$. These new operators may play an important role in tree-level dominated b decays in the general LRM.

The low-energy effects of the full theory at an arbitrary low-energy scale μ can then be described by the linear combination of the given operators and the corresponding Wilson coefficients (WCs) $C_i(\mu)$. In order to calculate $C_i(\mu)$, we first calculate them at $\mu = M_W$ scale. After performing a straightforward matching computation, we find the WCs including the electromagnetic penguin contributions at W scale neglecting the u -quark mass:

$$\begin{aligned} C_2^q(M_W) &= 1, & C_2^{q'}(M_W) &= \zeta_g \lambda_q^{RR} / \lambda_q^{LL} \quad (q = u, c), \\ C_3(M_W) &= \frac{\alpha}{6\pi \sin^2 \theta_W} [2B(x_t) + C(x_t)], \\ C_7(M_W) &= \frac{\alpha}{6\pi} [4C(x_t) + D(x_t)], \\ C_9(M_W) &= \frac{\alpha}{6\pi} \left[4C(x_t) + D(x_t) + \frac{1}{\sin^2 \theta_W} (10B(x_t) - 4C(x_t)) \right], \\ C_7^\gamma(M_W) &= F(x_t) + \frac{m_t}{m_b} A^{tb} \tilde{F}(x_t), & C_7^{\gamma'}(M_W) &= \frac{m_t}{m_b} A^{ts*} \tilde{F}(x_t), \\ C_8^G(M_W) &= G(x_t) + \frac{m_t}{m_b} A^{tb} \tilde{G}(x_t), & C_8^{G'}(M_W) &= \frac{m_t}{m_b} A^{ts*} \tilde{G}(x_t), \end{aligned} \quad (13)$$

$$C_{12}^u(M_W) = A^{ub}, \quad C_{12}^{u'}(M_W) = A^{us*},$$

where

$$x_U = \frac{m_U^2}{M_W^2} \quad (U = u, c, t), \quad A^{UD} = \xi_g \frac{V_{UD}^R}{V_{UD}^L} e^{i\alpha_o} \quad (D = b, s), \quad (14)$$

and α_o is a CP phase residing in the vacuum expectation values, which can be absorbed in α_i in Eq. (3) by redefining $\alpha_i + \alpha_o \rightarrow \alpha_i$. All other coefficients are negligible or vanish. In Eq. (13), the explicit forms of the functions $B(x_t)$, $C(x_t)$, and $D(x_t)$ can be found in Refs. [24, 25], and $F(x_t)$, $\tilde{F}(x_t)$, $G(x_t)$, and $\tilde{G}(x_t)$ are given in Ref. [26]. In the above magnetic coefficients, the terms proportional to ξ_g and ζ_g are neglected except the contribution coming from the virtual t quark which gives m_t/m_b enhancement. Also the term proportional to ζ_g in the coefficient C_2' is not neglected because $\zeta_g \geq \xi_g$ and there is possible enhancement by the ratio of CKM angles ($\lambda_q^{RR}/\lambda_q^{LL}$) in the nonmanifest LRM. Note that the new coefficient $C_{12}^{(l)'}(M_W)$ can be important in some $b \rightarrow s$ transitions because the ξ_g suppression can be offset by the ratio V_{uD}^R/V_{uD}^L in Eq. (14).

The coefficients $C_i(\mu)$ at the scale μ below m_b can be obtained by evolving the coefficients $C_i(M_W)$ with the 28×28 anomalous dimension matrix applying the usual renormalization group procedure in the following way:

$$\vec{C}(\mu) = U_4(\mu, m_b) M(m_b) U_5(m_b, M_W) \vec{C}(M_W), \quad (15)$$

where U_f is the evolution matrix for f active flavors and $M(m)$ gives the matching corrections between $\vec{C}_{f-1}(m)$ and $\vec{C}_f(m)$. In the leading logarithmic (LL) approximation $M = 1$ and the evolution matrix $U(m_1, m_2)$ is given by

$$U(m_1, m_2) = V \left[\left(\frac{\alpha_s(m_2)}{\alpha_s(m_1)} \right)^{\vec{\gamma}/2\beta_0} - \frac{\alpha}{2\beta_0} K(m_1, m_2) \right] V^{-1}, \quad (16)$$

where V diagonalizes the transposed of the anomalous dimension matrix γ_s and $\vec{\gamma}$ is the vector containing the eigenvalues of γ_s^T . In the right-hand side of Eq. (16), the first term represents the pure QCD evolution and the second term describes the additional evolution in the presence of the electromagnetic interaction. The leading order formula for the matrix $K(m_1, m_2)$ can be found in Refs. [24, 25]. Since the strong interaction preserves chirality, the 28×28 anomalous dimensional matrix decomposes into two identical 14×14 blocks. The SM 12×12 submatrix describing the mixing among $O_1 - O_{10}$, O_7^γ , and O_8^G can be found in Ref. [27], and the explicit form of the remaining 4×4 matrix describing the mixing among $O_{11,12}$, O_7^γ , and O_8^G , which partially overlaps with the SM 12×12 submatrix, can be found in Ref. [26].

In this paper, unlike the previous analysis in Ref. [19], we set the scale of weak WCs at $\mu = 1.5$ GeV to use the PQCD results for the hadronic matrix elements [28]. For 4 flavors, we have the following numerical values of $C_i(1.5$ GeV) in LL precision using the standard quark masses:¹

$$\begin{aligned} C_1^q &= -0.453, & C_1^{q'} &= C_1^q \zeta_g \lambda_q^{RR} / \lambda_q^{LL}, \\ C_2^q &= 1.231, & C_2^{q'} &= C_2^q \zeta_g \lambda_q^{RR} / \lambda_q^{LL}, \\ C_3 &= 0.024, & C_4 &= -0.046, & C_5 &= 0.012, & C_6 &= -0.066, \\ C_7 &= 0.014\alpha, & C_8 &= 0.069\alpha, & C_9 &= -1.436\alpha, & C_{10} &= 0.503\alpha, \\ C_7^\gamma &= -0.389 - 17.86A^{tb}, & C_7^{\gamma'} &= -17.86A^{ts*}, \\ C_8^G &= -0.177 - 7.858A^{tb}, & C_8^{G'} &= -7.858A^{ts*}. \end{aligned} \quad (17)$$

$$C_{11}^u = 0.641A^{ub}, \quad C_{12}^u = 0.879A^{ub}, \quad C_{11}^{u'} = 0.641A^{us*}, \quad C_{12}^{u'} = 0.879A^{us*},$$

where subdominant NP terms are neglected. Note that $C_3' - C_{10}'$ are negligible comparing to $C_7^{\gamma'}$ and $C_8^{G'}$ whereas $C_{1,2}'$ and $C_{11,12}^{(l)'}$ are not. $C_{1,2}^{(l)'}$ and $C_{11,12}^{(l)'}$ can be important especially to the tree-dominated B decays.

¹ Although QCD correction factors in $C_{1,2}'$ are different from those in $C_{1,2}$ in general, we use an approximation $\alpha_s(M_{W'}) \simeq \alpha_s(M_W)$ for simplicity, which will not change our result.

IV. $B \rightarrow K\pi$ DECAY AMPLITUDES

Following the procedure of Ref. [19] of including the penguin-type diagrams of the current-current operators $O_{1,2}$ and the tree-level diagrams associated with the magnetic operators O_7^γ and O_8^G , the one-loop matrix elements of \mathcal{H}_{eff} can be written in terms of the tree-level matrix elements of the effective operators:

$$\langle sq\bar{q}|\mathcal{H}_{eff}|B\rangle = -\frac{G_F}{\sqrt{2}}\lambda_t^{LL}\sum_{i=1}^{12}C_i^{eff}\langle sq\bar{q}|O_i|B\rangle^{tree} + (C_i^{eff}O_i \rightarrow C_i^{eff}O'_i), \quad (18)$$

with the effective WCs

$$\begin{aligned} C_i^{eff(\prime)} &= C_i^{(\prime)} \quad (i = 1, 2, 8, 10, 11, 12), \\ C_3^{eff(\prime)} &= C_3^{(\prime)} - \frac{1}{N_c}C_9^{(\prime)}, \quad C_4^{eff(\prime)} = C_4^{(\prime)} + C_9^{(\prime)}, \\ C_5^{eff(\prime)} &= C_5^{(\prime)} - \frac{1}{N_c}C_9^{(\prime)}, \quad C_6^{eff(\prime)} = C_6^{(\prime)} + C_9^{(\prime)}, \\ C_7^{eff(\prime)} &= C_7^{(\prime)} + C_\gamma^{(\prime)}, \quad C_9^{eff(\prime)} = C_9^{(\prime)} + C_\gamma^{(\prime)}, \end{aligned} \quad (19)$$

where

$$\begin{aligned} C_g^{(\prime)} &= -\frac{\alpha_s}{8\pi}\left[\frac{1}{\lambda_t^{LL}}\sum_{q=u,c}\lambda_q^{LL}C_2^{q(\prime)}\mathcal{I}(m_q, k, m_b) + 2C_8^{G(\prime)}\frac{m_b^2}{k^2}\right], \\ C_\gamma^{(\prime)} &= -\frac{\alpha}{3\pi}\left[\frac{1}{\lambda_t^{LL}}\sum_{q=u,c}\lambda_q^{LL}(C_1^{q(\prime)} + \frac{1}{N_c}C_2^{q(\prime)})\mathcal{I}(m_q, k, m_b) + C_7^{\gamma(\prime)}\frac{m_b^2}{k^2}\right], \end{aligned} \quad (20)$$

and

$$\mathcal{I}(m, k, \mu) = 4\int_0^1 dx x(1-x)\ln\left[\frac{m^2 - k^2x(1-x)}{\mu^2}\right]. \quad (21)$$

and where k is the momentum transferred by the photon or the gluon to the (q, \bar{q}) pair. Here k^2 is expected to be typically in the range $m_b^2/4 \leq k^2 \leq m_b^2/2$ [29], and we will use $k^2 = m_b^2/2$ for our numerical analysis. The expression of the decay amplitudes can be further simplified by combining the effective WCs in the following way:

$$a_{2i-1}^{(\prime)} = C_{2i-1}^{eff(\prime)} + \frac{1}{N_c}C_{2i}^{eff(\prime)}, \quad a_{2i}^{(\prime)} = C_{2i}^{eff(\prime)} + \frac{1}{N_c}C_{2i-1}^{eff(\prime)} \quad (i = 1, 2, 3), \quad (22)$$

where the factor $1/N_c$ originates from fierzing the operators $O_i^{(\prime)}$ after adopting the factorization assumption, and N_c is simply equal to the number of colors in the naive factorization approximation based on the vacuum-insertion method [30]. Also, in the PQCD approach, $N_c \approx 3$ as well because of the cancellation between the nonfactorizable contributions.

The matrix amplitudes for $B \rightarrow K\pi$ decays can then be written in terms of the effective WCs as

$$\begin{aligned} \mathcal{A}(\bar{B}^0 \rightarrow \pi^0 \bar{K}^0) &= \frac{G_F}{2}\left\{\left[\lambda_u^{LL}(a_1 + \rho_u^\pi a_{11}) + \frac{3}{2}\lambda_t^{LL}(a_7 - a_9)\right]X^{(BK, \pi)}\right. \\ &\quad + \lambda_t^{LL}\left[a_4 - \frac{1}{2}a_{10} + 2\rho_s^K\left(a_6 - \frac{1}{2}a_8\right)\right]X^{(B\pi, K)} \\ &\quad + \lambda_t^{LL}\left[a_4 - \frac{1}{2}a_{10} + 2\rho_s^B\left(a_6 - \frac{1}{2}a_8\right)\right]X^{(B, \pi K)}\left.\right\} \\ &\quad + (a_i \rightarrow -a'_i), \quad (23) \\ \mathcal{A}(\bar{B}^0 \rightarrow \pi^+ K^-) &= \frac{G_F}{\sqrt{2}}\left\{\left[\lambda_u^{LL}(a_2 + a_{12}) - \lambda_t^{LL}\left(a_4 + a_{10} + 2\rho_s^K(a_6 + a_8)\right)\right]X^{(B\pi, K)}\right. \\ &\quad \left.- \lambda_t^{LL}\left[a_4 - \frac{1}{2}a_{10} + 2\rho_s^B\left(a_6 - \frac{1}{2}a_8\right)\right]X^{(B, \pi K)}\right\} \end{aligned}$$

$$+(a_i \rightarrow -a'_i), \quad (24)$$

$$\begin{aligned} \mathcal{A}(B^- \rightarrow \pi^0 K^-) = & \frac{G_F}{2} \left\{ \left[\lambda_u^{LL}(a_1 + \rho_u^\pi a_{11}) + \frac{3}{2} \lambda_t^{LL}(a_7 - a_9) \right] X^{(BK,\pi)} \right. \\ & + \left[\lambda_u^{LL}(a_2 + a_{12}) - \lambda_t^{LL}(a_4 + a_{10} + 2\rho_s^K(a_6 + a_8)) \right] X^{(B\pi,K)} \\ & + \left. \left[\lambda_u^{LL}(a_2 - a_{12}) - \lambda_t^{LL}(a_4 + a_{10} + 2\rho_s^B(a_6 + a_8)) \right] X^{(B,\pi K)} \right\} \\ & + (a_i \rightarrow -a'_i), \quad (25) \end{aligned}$$

$$\begin{aligned} \mathcal{A}(B^- \rightarrow \pi^- \bar{K}^0) = & \frac{G_F}{\sqrt{2}} \left\{ -\lambda_t^{LL} \left[a_4 - \frac{1}{2} a_{10} + 2\rho_s^K \left(a_6 - \frac{1}{2} a_8 \right) \right] X^{(B\pi,K)} \right. \\ & + \left. \left[\lambda_u^{LL}(a_2 - a_{12}) - \lambda_t^{LL}(a_4 + a_{10} + 2\rho_s^B(a_6 + a_8)) \right] X^{(B,\pi K)} \right\} \\ & + (a_i \rightarrow -a'_i), \quad (26) \end{aligned}$$

where

$$\begin{aligned} X^{(BK,\pi)} &= -\sqrt{2} \langle \pi^0 | \bar{u} \gamma^\mu \gamma_5 u | 0 \rangle \langle \bar{K}^0 | \bar{s} \gamma_\mu b | \bar{B}^0 \rangle \\ &= i f_\pi F_0^{B \rightarrow K}(m_\pi^2)(m_B^2 - m_K^2), \\ X^{(B\pi,K)} &= +\sqrt{2} \langle \bar{K}^0 | \bar{s} \gamma^\mu \gamma_5 d | 0 \rangle \langle \pi^0 | \bar{d} \gamma_\mu b | \bar{B}^0 \rangle \\ &= i f_K F_0^{B \rightarrow \pi}(m_K^2)(m_B^2 - m_\pi^2), \\ X^{(B,\pi K)} &= +\sqrt{2} \langle \pi^0 \bar{K}^0 | \bar{s} \gamma^\mu d | 0 \rangle \langle 0 | \bar{d} \gamma_\mu \gamma_5 b | \bar{B}^0 \rangle \\ &= i f_B F_0^{\pi K}(m_B^2)(m_K^2 - m_\pi^2), \quad (27) \end{aligned}$$

and where

$$\rho_q^H \equiv \frac{m_H^2}{m_b m_q} \quad (H = \pi, K, B, \quad q = u, s). \quad (28)$$

Note from Eq. (27) that the form factors $F_0^{B \rightarrow K}$ and $F_0^{B \rightarrow \pi}$ can be determined by relevant semileptonic B decays, but $F_0^{\pi K}$ is not. Because of the significant hadronic uncertainties in the factorization approximation of the matrix amplitudes, it is very difficult to separately determine the size of NP contributions. Therefore, in this paper, instead of performing a complete analysis by varying all relevant independent NP parameters ($\zeta_g, \xi_g, \theta_R, \alpha_{2,3,4}$) in this model, we fix ξ_g and $\alpha_{1,3,4}$ for simple illustration of NP effects. Also, for numerical analysis, we use the following values of form factors obtained from PQCD calculation [31]:

$$F_0^{B \rightarrow K}(m_\pi^2) = 0.37, \quad F_0^{B \rightarrow \pi}(m_K^2) = 0.24, \quad F_0^{\pi K}(m_B^2) = (0.39 + 8.16i)10^{-4}. \quad (29)$$

The form factor $F_0^{\pi K}(m_B^2)$ which originates from annihilation contributions is complex due to the final state quark interactions, so that it could be important in CP observables. Also, due to the enhancement factor ρ_s^B proportional to m_B^2 , the annihilation contributions are not negligible.

V. RESULTS

For illustration of allowed new model parameter spaces, we first fix the new gauge boson mass to be $M_{W'} = (g_R/g_L) \times 1.5$ TeV, and plot the allowed region of α_2 and θ_R at 2σ level for $\alpha_1 = \alpha_3 = \pi$ in Fig. 1(a) and for $\alpha_1 = \pi, \alpha_3 = -\pi/2$ in Fig. 1(b) using the present experimental bounds of the CP asymmetries in Eq. (1). With the chosen NP parameters, the branching fraction of each decay mode in Eq. (23) agrees with the present experimental measurement as well. In Fig. 1, the region (nearly all) above the dotted line is allowed by the V_{ub} bound given in Eq. (6), and the shaded area inside the dashed lines is allowed by the $B_s^0 - \bar{B}_s^0$ mixing bound in Eq. (10). From the overlapped allowed regions of the figures, one can see that the value of θ_R could be either small or large, but nonzero value of α_2 near 60° is preferred in both cases similarly.

In order to clearly see W' mass dependence, we plot the allowed region of θ_R and ζ_g at 2σ level for $\alpha_2 = 55^\circ$ in Fig. 2, taking into account the constraint from the muon decay measurements given in Eq. (4). In Fig. 2, similarly, the shaded regions left of the dotted and dashed lines are allowed by the V_{ub} bound given in Eq. (6) and by the

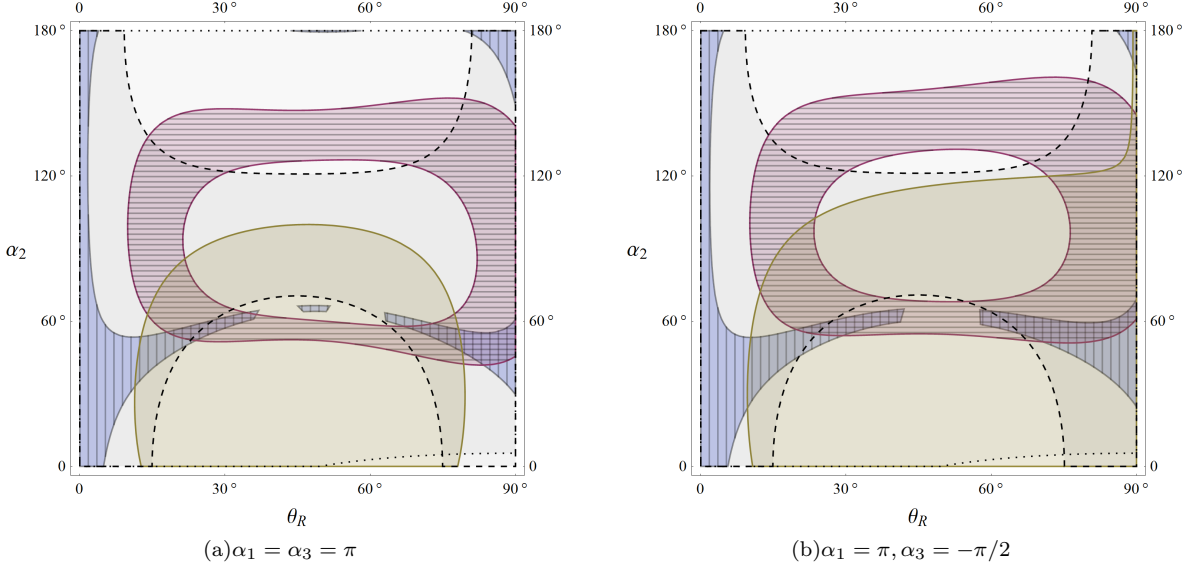


FIG. 1: Allowed regions for α_2 and θ_R at 2σ level for $M_{W'} = (g_R/g_L) \times 1.5$ TeV. The blue(vertical mesh), red(horizontal mesh), and yellow(no mesh) regions are allowed by the current measurements of $A_{CP}(B^0 \rightarrow K^\pm \pi^\mp)$, $A_{CP}(B^\pm \rightarrow K^\pm \pi^0)$, and $A_{CP}(B^\pm \rightarrow K^0 \pi^\pm)$, respectively. The dotted and dashed lines indicate the bounds by the measurements of V_{ub} and $B_s^0 - \bar{B}_s^0$ mixing, respectively.

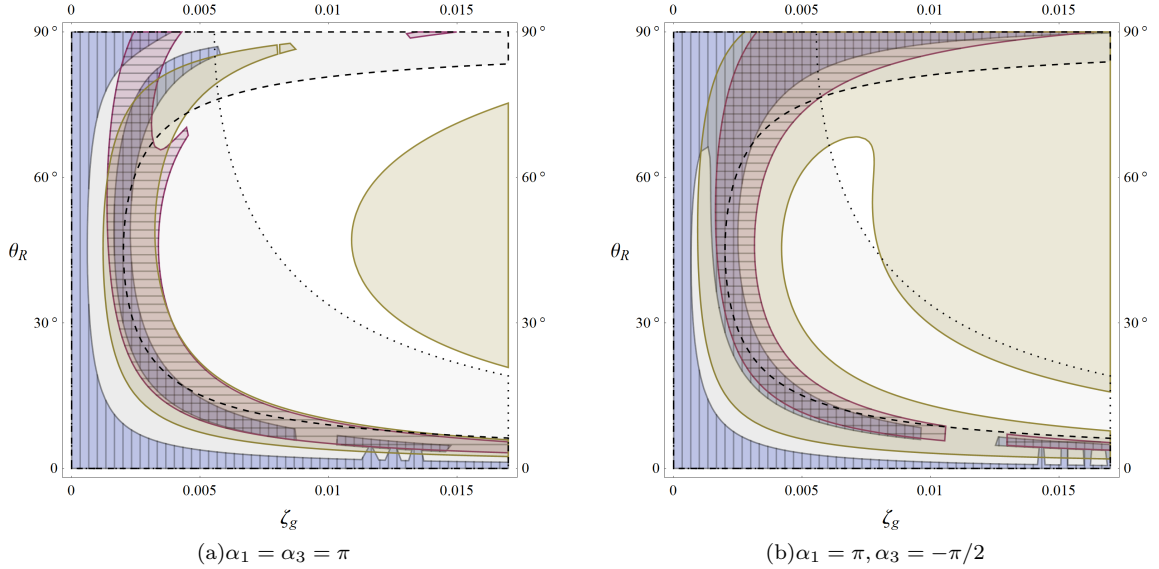


FIG. 2: Allowed regions for θ_R and ζ_g at 2σ level. The blue(vertical mesh), red(horizontal mesh), and yellow(no mesh) regions are allowed by the current measurements of $A_{CP}(B^0 \rightarrow K^\pm \pi^\mp)$, $A_{CP}(B^\pm \rightarrow K^\pm \pi^0)$, and $A_{CP}(B^\pm \rightarrow K^0 \pi^\pm)$, respectively. The dotted and dashed lines indicate the bounds by the measurements of V_{ub} and $B_s^0 - \bar{B}_s^0$ mixing, respectively.

$B_s^0 - \bar{B}_s^0$ mixing bound in Eq. (10), respectively. With the given parameter sets, we estimate the size of the right-handed current contributions responsible for the present measurements of $A_{CP}(B^0 \rightarrow K^\pm \pi^\mp)$, $A_{CP}(B^\pm \rightarrow K^\pm \pi^0)$, and $A_{CP}(B^\pm \rightarrow K^0 \pi^\pm)$ as shown in Fig. 2, and obtain the lower bound of ζ_g approximately given as $\zeta_g \gtrsim 0.0015$ which corresponds to the upper bound of W' mass $M_{W'} \lesssim (g_R/g_L) \times 2.1$ TeV. We found that this mass bound could be somewhat higher for different values of α_2 , but not drastically different. It should also be noted that we scanned other sets of NP parameters, and have no better results (no wider simultaneously allowed regions) for different values of $\alpha_{1,3,4}$.

VI. CONCLUDING REMARKS

In this paper, we studied the right-handed current contributions to the direct CP asymmetries in $B \rightarrow K\pi$ decays taking into account all possible tree and penguin contributions including annihilation-type amplitudes by adopting PQCD approach in the nonmanifest LRM. Without imposing manifest or pseudomanifest left-right symmetry, we parametrized V^R as shown in Eq. (3) so that W' mass is not strongly constrained by the current direct and indirect search results [13, 18], and showed that the CP asymmetries are sensitive to the phases and angles in V^R as well as to the mass of W' . We considered the constraints from the global analysis of muon decay parameters, the determination of $|V_{ub}|$ in inclusive and exclusive B decays, and $B_s^0 - \bar{B}_s^0$ mixing measurements. With the given phases, one can see from the figures that relatively large value of the mixing angle θ_R is preferred unless W' mass is as light as a few hundred GeV. This could also give simultaneous explanations to the large branching fractions of $B \rightarrow \tau\nu$ transitions due to a large fraction V_{ub}^R/V_{ub}^L [17], and also to the large CP-violating like-sign dimuon charge asymmetry in semileptonic B decays [20] due to a large CP-violating phase in B_s mixing [18]. Also, with the given parameter sets, Fig. 2 shows that it is favorable that the mass of W' is lighter than around $(g_R/g_L) \times 2.1$ TeV in order to incorporate the current experimental measurements. In this way, CP asymmetries in other nonleptonic B decays such as $B \rightarrow K\rho$ and $B \rightarrow K^*\pi$ can be estimated systematically and similarly, and all of these analysis of possible NP contributions can be tested once future experimental progress can further improve the bounds.

Acknowledgments

S.-h. Nam thanks C.-H. Chen and H.-n. Li for useful communications, and C.-W. Chiang for collaboration at the beginning of this project. The computation of this work was supported in part by the PLSI supercomputing resources of KISTI.

-
- [1] For a recent review, for example, see S. Mishima, arXiv:1101.1501 [hep-ph].
 - [2] Heavy Flavor Averaging Group, <http://www.slac.stanford.edu/xorg/hfag/>.
 - [3] A. Ali, G. Kramer, and C.-D. Lü, Phys. Rev. D **59**, 014005 (1998).
 - [4] S. Baek, C.-W. Chiang, and D. London, Phys. Lett. B **675**, 59 (2009).
 - [5] M. Gronau, O.F. Hernandez, D. London, and J.L. Rosner, Phys. Rev. D **50**, 4529 (1994); *ibid.* **52**, 6374 (1995).
 - [6] M. Beneke and M. Neubert, Nucl. Phys. B **675**, 333 (2003); H.Y. Cheng and K.C. Yang, Phys. Rev. D **78**, 094001 (2008); *ibid.* **79**, 039903 (2009).
 - [7] H.-n. Li, S. Mishima, and A.I. Sanda, Phys. Rev. D **72**, 114005 (2005); H.-n. Li and S. Mishima, Phys. Rev. D **73**, 114014 (2006); *ibid.* **83**, 034023 (2011).
 - [8] C.W. Bauer, I.Z. Rothstein, and I.W. Stewart, Phys. Rev. D **74**, 034010 (2006); M. Duraismy and A. Kagan, Eur. Phys. J. C **70**, 921 (2010).
 - [9] A.J. Buras, R. Fleischer, S. Recksiegel, and F. Schwab, Eur. Phys. J. C **32**, 45 (2003); V. Barger, C.-W. Chiang, P. Langacker, and H.-S. Lee, Phys. Lett. B **598**, 218 (2004); R. Arnowitt, B. Dutta, B. Hu, and S. Oh, Phys. Lett. B **633**, 748 (2006); Y.-D. Yang, R. Wang, and G.R. Lu, Phys. Rev. D **73**, 015003 (2006); M. Imbeault, S. Baek, and D. London, Phys. Lett. B **663**, 410 (2008); S. Baek *et al.*, Phys. Lett. B **678**, 97 (2009); S. Chang, C.S. Kim, and J. Song, Phys. Lett. B **696**, 367 (2011); J.N. Ng and P.T. Winslow, JHEP **1202**, 140 (2012).
 - [10] R. N. Mohapatra and J. C. Pati, Phys. Rev. D **11**, 2558 (1975); J. C. Pati and A. Salam, Phys. Rev. D **10**, 275 (1974); Erratum *ibid.* D **11**, 703 (1975); For a review, see R. N. Mohapatra, *Unification and Supersymmetry* (Springer, New York, 1986).
 - [11] J. Chay, K.Y. Lee, and S.-h. Nam, Phys. Rev. D **61**, 035002 (1999).
 - [12] D. Chang, J. Basecq, L.-F. Li, and P.B. Pal, Phys. Rev. D **30**, 1601 (1984).
 - [13] P. Langacker and S.U. Sankar, Phys. Rev. D **40**, 1569 (1989); J. Erler, and P. Langacker, Phys. Lett. B **456**, 68 (1999).
 - [14] Y. Zhang *et al.*, Phys. Rev. D **76**, 091301 (2007).
 - [15] V. Khachatryan *et al.* (CMS Collaboration), Phys. Lett. B **698**, 21 (2011); S. Chatrchyan *et al.* (CMS Collaboration), Phys. Lett. B **701**, 160 (2011); G. Aad *et al.* (ATLAS Collaboration), Phys. Lett. B **701**, 50 (2011). G. Aad *et al.* (ATLAS Collaboration), Phys. Lett. B **705**, 28 (2011).
 - [16] T. G. Rizzo, Phys. Rev. D **58**, 114014 (1998).
 - [17] C.-H. Chen and S.-h. Nam, Phys. Lett. B **666**, 462 (2008).
 - [18] A.J. Buras, K. Gemmler, and G. Isidori, Nucl. Phys. B **843**, 107 (2011).
 - [19] S.-h. Nam, Phys. Rev. D **68**, 115006 (2003).
 - [20] K.Y. Lee and S.-h. Nam, Phys. Rev. D **85**, 035001 (2012).
 - [21] A. Hillairet *et al.*, Phys. Rev. D **85**, 092013 (2012).
 - [22] S.-h. Nam, Phys. Rev. D **66**, 055008 (2002).

- [23] A. Lenz *et al.*, Phys. Rev. D **86**, 033008 (2012).
- [24] G. Buchalla, A.J. Buras, and M. Lautenbacher, Rev. Mod. Phys. **68**, 1125 (1996); A.J. Buras, hep-ph/9806471.
- [25] G. Buchalla, A.J. Buras, and M.K. Harlander, Nucl. Phys. B **337**, 313 (1990).
- [26] P. Cho and M. Misiak, Phys. Rev. D **49**, 5894 (1994).
- [27] M. Ciuchini *et al.*, Phys. Lett. B **316**, 127 (1993); Nucl. Phys. B **415**, 403 (1994); also see Ref. [24] .
- [28] Y.-Y. Keum, H.-n. Li, and A.I. Sanda, Phys. Rev. D **63**, 054008 (2001).
- [29] J.-M. Gérard and W.-S. Hou, Phys. Rev. Lett. **62**, 855 (1989); *ibid.*, Phys. Rev. D **43**, 2909 (1991); N.G. Deshpande and J. Trampetic, Phys. Rev. D **41**, 2926 (1990); H. Simma and D. Wyler, Phys. Lett. B **272**, 395 (1991).
- [30] M.K. Gaillard and B.W. Lee, Phys. Rev. D **10**, 897 (1974).
- [31] C.-H. Chen and H. Hatanaka, Phys. Rev. D **73**, 075003 (2006).